Local Time-domain Spherical Harmonic Spatial Encoding for Wave-based Acoustic Simulation

Local Time-domain Spherical Harmonic Spatial Encoding for Wave-based Acoustic Simulation

Stefan Bilbao, *Senior Member, IEEE,* Archontis Politis, *Member, IEEE* and Brian Hamilton, *Member, IEEE*

***Abstract*—Volumetric time-domain simulation methods, such as the finite difference time domain (FDTD) method, allow for a fine-grained representation of the dynamics of the acoustic field. A key feature of such methods is complete access to the computed field, normally represented over a Cartesian grid. Simple solutions to the problem of extracting spatially-encoded signals, necessary in virtual acoustics applications, result. In this article, a simple time domain representation of spatially-encoded spherical harmonic signals is written directly in terms of spatial derivatives of the acoustic field at the receiver location. In a discrete setting, encoded signals may be obtained, at very low computational cost and latency, using local approximations with minimal number of grid points, and avoiding large convolutions and frequency-domain block processing of previous approaches. Numerical results illustrating receiver directivity and computed time domain responses are presented, as well as numerical solution drift associated with repeated time integration.**

***Index Terms*—FDTD, room acoustics, spatial audio, microphone array, spherical harmonics, ambisonics.**

I. Introduction

Wave-based volumetric time-domain simulation for virtual acoustics dates back to the 1990s [1]–[3] and relies on a time domain numerical solution to the 3D wave equation over a spatial grid. Various interlinked methodologies, including the finite difference time domain (FDTD) [4]–[6], finite volume time domain (FVTD) [7], [8], waveguide mesh [9] and pseudospectral methods [10] have been proposed. A key feature of such volumetric time-domain methods is that the calculated acoustic field is available in its entirety, and thus the modeling of locally-defined objects (including sources and receivers) is reduced to simple locally-defined operations over the grid.

Spatial encoding of simulation output is a necessary step towards full virtual acoustic auralisation. A good candidate is the Ambisonics framework [11], [12], which can be decoded to arbitrary playback systems [13], [14]. For wave-based volumetric methods, previous approaches have followed from those used in spatial recording. Spherical array processing [15], [16] was employed for 3D ambisonic encoding in [17] and differential microphone processing [18], [19] was used in [20] to obtain 2D ambisonic signals. An alternative approach is through plane wave decomposition [21], [22]. These approaches [17], [21], [22] rely on pre-computation of encoding filters, implementing a frequency-domain inversion from pressure values to the encoded signals, and applied to grid signals using block-processing frequency-domain techniques.

In this work, instead of following the array processing paradigm, the encoding process is formulated and integrated directly in the FDTD scheme, operating with very low latency and without extensive pre-computation. We demonstrate that this is possible through the relation between spherical harmonic encoding and the local pressure gradients of the sound-field, through a representation first presented by Dickins and Kennedy [23], and also employed in non-volumetric frequency-domain techniques by Mehra et al. [24]. In the present setting of volumetric time-domain methods, the resulting procedure selects explicit compact grid point sets for each encoded signal and is recursive in the time-domain.

In Section II, spatially-encoded signals for the acoustic field are defined for a given receiver location, and written directly in the spatio-temporal domain. Finite difference time domain schemes for the 3D wave equation are introduced in Section III, followed by basic local approximations to the encoded signals, which may be retrieved from the acoustic field through low-order recursions. Numerical results appear in Section IV.

II. Spatial Sound Field Encoding

Under free field conditions, the pressure distribution in an enclosure is assumed to satisfy the 3D wave equation [25]:

$$\left(1/c^2\right) \partial_t^2 p(\mathbf{r},t) = \Delta p(\mathbf{r},t) \quad . \tag{1}$$

Here, $p\left(\mathbf{r},t\right)$ is the pressure distribution in Pa, as a function of time t and a spatial coordinate $\mathbf{r} = [x,y,z]$. c is the wave speed, in $\mathrm{m{\cdot}s^{-1}}$, and ∂_t represents partial differentiation with respect to time t. $\Delta = \nabla \cdot \nabla$ is the 3D Laplacian operator, written in terms of the 3D gradient operation, defined by

$$\nabla = [\partial_x, \partial_y, \partial_z] \quad , \tag{2}$$

where ∂_ν represents partial spatial differentiation with respect to coordinate ν, $\nu = x,y,z$.

Under Fourier transformation, $p\left(\mathbf{r},t\right) \longrightarrow \hat{p}\left(\mathbf{r},\omega\right)$, where ω is angular frequency, and (1) reduces to Helmholtz's equation:

$$-\left(\omega^2/c^2\right) \hat{p}(\mathbf{r},\omega) = \Delta \hat{p}(\mathbf{r},\omega) \quad . \tag{3}$$

A general solution is a plane wave superposition [16]:

$$\hat{p}\left(\mathbf{r},\omega\right) = \int_{S^2} \hat{a}\left(\boldsymbol{\gamma},\omega\right) e^{i\frac{\omega}{c}\boldsymbol{\gamma}\cdot\mathbf{r}} d\Omega \quad . \tag{4}$$

Here, the unit sphere S^2 is parameterized by the angle pair (α,β), $0 \leq \alpha < 2\pi$, and $0 \leq \beta \leq \pi$. The surface differential element $d\Omega = \sin\beta d\beta d\alpha$, and the unit-length vector $\boldsymbol{\gamma}$ is

$$\boldsymbol{\gamma} = [\gamma_x, \gamma_y, \gamma_z] = [\cos\alpha \sin\beta, \sin\alpha \sin\beta, \cos\beta] \quad . \tag{5}$$

This work was supported by the European Research Council, under grant number ERC-2016-PoC-737574-WRAM.

S. Bilbao and B. Hamilton are with the Acoustics and Audio Group, University of Edinburgh, Edinburgh EH9 3JZ, UK (e-mail: sbilbao@staffmail.ed.ac.uk).

A. Politis is with the Faculty of Information Technology and Communication Sciences, Tampere University, Aalto University, FI-00076 AALTO, Espoo, Finland (e-mail: archontis.politis@aalto.fi).

TABLE I
$Y_{l,m}(\boldsymbol{\gamma})$ FOR $l = 0, 1, 2$.

$m \backslash l$	0	1	2
-2	·	·	$\sqrt{15/4\pi}\gamma_x\gamma_y$
-1	·	$\sqrt{3/4\pi}\gamma_y$	$\sqrt{15/4\pi}\gamma_y\gamma_z$
0	$\sqrt{1/4\pi}$	$\sqrt{3/4\pi}\gamma_z$	$\sqrt{5/16\pi}\left(2\gamma_z^2-\gamma_x^2-\gamma_y^2\right)$
1	·	$\sqrt{3/4\pi}\gamma_x$	$\sqrt{15/4\pi}\gamma_x\gamma_z$
2	·	·	$\sqrt{15/16\pi}\left(\gamma_x^2-\gamma_y^2\right)$

$\hat{a}(\boldsymbol{\gamma},\omega)$ represents the wave amplitude density at frequency ω, and with direction of incidence $\boldsymbol{\gamma}$. It may be decomposed into spherical harmonics $Y_{l,m}$ with coefficients $\hat{a}_{l,m}(\omega)$ as

$$\hat{a}(\boldsymbol{\gamma},\omega) = \sum_{l=0}^{\infty}\sum_{m=-l}^{l} \hat{a}_{l,m}(\omega)\, Y_{l,m}(\boldsymbol{\gamma}) \quad . \tag{6}$$

Obtaining the coefficients $\hat{a}_{l,m}(\omega)$ forms the basis of ambisonic recording. By convention in Ambisonics, real spherical harmonics $Y_{l,m}$ are assumed here, of order $l = 0, \ldots, \infty$ and degree $m = -l, \ldots, l$, that are orthonormal over S^2:

$$\int_{S^2} Y_{l,m}(\boldsymbol{\gamma})\, Y_{l',m'}(\boldsymbol{\gamma})\, d\Omega = \begin{cases} 1, & l = l', m = m' \\ 0, & \text{otherwise} \end{cases} \quad . \tag{7}$$

Equations (4) and (6) may be combined to yield

$$\hat{p}(\mathbf{r},\omega) = \sum_{l=0}^{\infty}\sum_{m=-l}^{l} \hat{a}_{l,m}(\omega) \int_{S^2} Y_{l,m}(\boldsymbol{\gamma})\, e^{i\frac{\omega}{c}\boldsymbol{\gamma}\cdot\mathbf{r}} d\Omega \quad . \tag{8}$$

Through a direct evaluation of (8), one may arrive at the more familiar Fourier-Bessel expansion for the acoustic field [26]:

$$\hat{p}(\mathbf{r},\omega) = 4\pi \sum_{l=0}^{\infty}\sum_{m=-l}^{l} i^l j_l(\omega r/c)\, Y_{l,m}(\hat{\mathbf{r}})\, a_{l,m}(\omega) \quad , \tag{9}$$

where $r = |\mathbf{r}|$ and $\hat{\mathbf{r}} = \mathbf{r}/r$, and j_l is the lth order spherical Bessel function. The form in (8), however, is a good starting point for spatio-temporal series representations of the field, useful in an FDTD setting. See Section III.

The spherical harmonic $Y_{l,m}(\boldsymbol{\gamma})$, when written in terms of the components γ_x, γ_y and γ_z of the unit length vector $\boldsymbol{\gamma}$, is a homogeneous polynomial of degree l. Explicit forms for $Y_{l,m}$, up to order $l = 2$, are as shown in Table I. A corresponding spatial differential operator $D_{l,m}$ may be defined by

$$D_{l,m} = Y_{l,m}(\nabla) \quad , \tag{10}$$

also a polynomial, now in the components of the gradient operation defined in (2). For example, $D_{2,2} = \sqrt{\frac{15}{16\pi}}\left(\partial_x^2 - \partial_y^2\right)$.

A. Acoustic Field Derivatives

The Taylor expansion has been studied mostly in the context of differential array processing [19], [27]. In sound field recording, where the Fourier-Bessel expansion is more commonly used, relations between the terms of the two expansions were given by Cotterell up to 2nd order [28] and by Dickins for the general case [29]. Additionally, [30] exploited this relation to express room transfer functions for directional receivers.

Applying the spatial differential operator $D_{l',m'}$, as defined in (10), to the representation in (8) leads to

$$D_{l',m'}\hat{p} = \sum_{l=0}^{\infty}\sum_{m=-l}^{l} \hat{a}_{l,m}(\omega) \int_{S^2} Y_{l,m}(\boldsymbol{\gamma})\, D_{l',m'} e^{i\frac{\omega}{c}\boldsymbol{\gamma}\cdot\mathbf{r}} d\Omega \quad . \tag{11}$$

But, using

$$D_{l',m'} e^{i\frac{\omega}{c}\boldsymbol{\gamma}\cdot\mathbf{r}} = (i\omega/c)^{l'}\, Y_{l',m'}(\boldsymbol{\gamma})\, e^{i\frac{\omega}{c}\boldsymbol{\gamma}\cdot\mathbf{r}} \quad , \tag{12}$$

and evaluating (11) at $\mathbf{r} = \mathbf{0}$ gives

$$\left(D_{l',m'}\hat{p}\right)|_{(\mathbf{0},\omega)} = (i\omega/c)^{l'} \sum_{l=0}^{\infty}\sum_{m=-l}^{l} \hat{a}_{l,m}(\omega) \int_{S^2} Y_{l,m}(\boldsymbol{\gamma})\, Y_{l',m'}(\boldsymbol{\gamma})\, d\Omega \quad . \tag{13}$$

Employing the orthonormality of $Y_{l,m}$, from (7), yields

$$(i\omega/c)^{l}\, \hat{a}_{l,m} = \left(D_{l,m}\hat{p}\right)|_{(\mathbf{0},\omega)} \quad . \tag{14}$$

This expression appears in Dickins [29].

Inverse Fourier transforming to the time domain gives

$$(d/dt)^{l}\, a_{l,m} = c^{l}\left(D_{l,m}p\right)|_{(\mathbf{0},t)} \quad . \tag{15}$$

The representation in (15) is expressed directly in the spatio-temporal domain, as a relation between the lth time derivative of a given expansion coefficient $a_{l,m}(t)$ and an lth order combination of spatial derivatives of the acoustic field $p(\mathbf{r},t)$ at $\mathbf{r} = \mathbf{0}$. It is also exact, and can be viewed as a convenient context-free starting point for discretisation, regardless of the particular configuration of the spatial grid.

III. Finite Difference Time Domain Methods

Finite difference time domain methods for the wave equation are covered in a variety of sources [31]. For the sake of brevity, only the most basic scheme will be presented here.

First, assume a spatial grid, with spacing X and indexed by the integer-valued 3-vector $\mathbf{q} = [q_x, q_y, q_z]$. The grid function $p_{\mathbf{q}}^n$ represents an approximation to $p(\mathbf{r},t)$ at $\mathbf{r} = \mathbf{q}X$ and $t = nT$ for integer n and time step T. A two-step explicit scheme for the 3D wave equation (1) has the form

$$p_{\mathbf{q}}^{n+1} = 2p_{\mathbf{q}}^n - p_{\mathbf{q}}^{n-1} + \lambda^2 \sum_{\boldsymbol{\nu}\in\mathbb{Q}} \left(p_{\mathbf{q}+\boldsymbol{\nu}}^n - p_{\mathbf{q}}^n\right) \quad . \tag{16}$$

Here, $\mathbb{Q} = \{\mathbf{q} \in \mathbb{Z}^3 | \|\mathbf{q}\|_1 = 1\}$ defines the nearest neighbour stencil of the scheme, and $\lambda = cT/X$ is the Courant number [32] for the scheme. For numerical stability, the Courant-Friedrichs-Lewy condition $\lambda \leq 1/\sqrt{3}$ must be satisfied.

A plane wave solution satisfying (16) is of the form

$$p_{\mathbf{q}}^n = e^{i\left(\tilde{\omega}nT + \tilde{\mathbf{k}}\cdot\mathbf{q}X\right)} \quad , \tag{17}$$

where $\tilde{\omega}$ and $\tilde{\mathbf{k}} = \tilde{k}\boldsymbol{\gamma}$ are the numerical angular frequency and wave vector, respectively, where $\tilde{k}$ is the numerical wavenumber. They are related by the numerical dispersion relation

$$\tilde{\omega} = \frac{2}{T}\sin^{-1}\left(\lambda\sqrt{\sum\nolimits_{\nu=x,y,z}\sin^2\left(\tilde{k}\gamma_\nu X/2\right)}\right) \quad . \tag{18}$$

Note that $\tilde{\omega} \neq c\tilde{k}$, and thus wave speed is dependent on frequency and direction. Above a cutoff frequency $\tilde{\omega}_c =$

$(2/T)\sin^{-1}(\lambda)$ the scheme does not support wave propagation in all directions; below this cutoff, (18) may be inverted numerically to determine an expression $\tilde{k}(\tilde{\omega}, \boldsymbol{\gamma})$ for wavenumber in terms of frequency and direction.

A. Difference Operators and Recursion

The representation (15) is a set of differential equations, driven by data obtained from the acoustic field derivatives. It may be approximated numerically as a recursion. First, define $a^n_{l,m}$, approximating $a_{l,m}(t)$ at $t = nT$, for integer n. Forward and backward shift operators s^+_t and s^-_t are defined through $s^+_t a^n_{l,m} = a^{n+1}_{l,m}$ and $s^-_t a^n_{l,m} = a^{n-1}_{l,m}$. Forward and backward approximations δ^+_t and δ^-_t to the time derivative d/dt, and a backward averaging operator μ^-_t may be written as

$$\delta^+_t = \frac{1}{T}\left(s^+_t - 1\right) \quad \delta^-_t = \frac{1}{T}\left(1 - s^-_t\right) \quad \mu^-_t = \frac{1}{2}\left(1 + s^-_t\right) \quad . \tag{19}$$

A given order $l \geq 0$ may be written as $l = 2N + \alpha$, for integer $N \geq 0$ and $\alpha \in \{0, 1\}$. Basic approximations to the lth time derivative d^l/dt^l may be written as

$$\delta^{(\min)}_{t,l} = \left(\delta^+_t\right)^{N+\alpha}\left(\delta^-_t\right)^N \quad \delta^{(\circ)}_{t,l} = \left(\mu^-_t\right)^\alpha \delta^{(\min)}_{t,l} \quad . \tag{20}$$

$\delta^{(\min)}_{t,l}$ is minimal in terms of the number of time steps employed, but is non-centered (forward biased) for odd l. $\delta^{(\circ)}_{t,l}$ is centered for all l, but not minimal.

Equation (15) requires the approximation of lth order spatial derivatives of the acoustic field at $\mathbf{r} = \mathbf{0}$, corresponding to grid location $\mathbf{q} = \mathbf{0}$. The differential operator $D_{l,m}$ is homogeneous of degree l, and thus may be represented as

$$D_{l,m} = \sum_{\boldsymbol{\xi} \in \mathbb{V}_l} \sigma^{(\boldsymbol{\xi})}_{l,m} \partial_x^{\xi_x} \partial_y^{\xi_y} \partial_z^{\xi_z} \quad , \tag{21}$$

where $\mathbb{V}_l$ is the set of non-negative integer-valued 3-vectors $\boldsymbol{\xi} = [\xi_x, \xi_y, \xi_z]$ whose components sum to l, and $\sigma^{(\boldsymbol{\xi})}_{l,m}$, $\boldsymbol{\xi} \in \mathbb{V}_l$ are associated coefficients.

For a given coordinate ν, $\nu = x, y, z$, unit forward and backward shifts s^+_ν and s^-_ν may be defined, through their operation on the grid function $p^n_{\mathbf{q}}$ as $s^+_\nu p^n_{\mathbf{q}} = p^n_{\mathbf{q}+\mathbf{e}_\nu}$ and $s^-_\nu p^n_{\mathbf{q}} = p^n_{\mathbf{q}-\mathbf{e}_\nu}$, where $\mathbf{e}_\nu$ is a unit vector in the ν direction. As before, forward and backward difference operators approximating ∂_ν are defined by

$$\delta^+_\nu = \frac{1}{X}\left(s^+_\nu - 1\right) \quad \delta^-_\nu = \frac{1}{X}\left(1 - s^-_\nu\right) \quad \mu^-_\nu = \frac{1}{2}\left(1 + s^-_\nu\right) \quad . \tag{22}$$

As above, minimal and centered difference approximations to δ^ξ_ν, for integer $\xi \geq 0$, decomposable uniquely as $\xi = 2M + \gamma$, for integer $M \geq 0$, and $\gamma \in \{0, 1\}$, may be defined as

$$\delta^{(\min)}_{\nu,\xi} = \left(\delta^+_\nu\right)^{M+\gamma}\left(\delta^-_\nu\right)^M \quad \delta^{(\circ)}_{\nu,\xi} = \left(\mu^-_\nu\right)^\gamma \delta^{(\min)}_{\nu,\xi} \quad . \tag{23}$$

Approximations to the differential operator $D_{l,m}$, in the form given in (21), may be written as

$$\delta^{(\cdot)}_{\mathbf{r},l,m} = \sum_{\boldsymbol{\xi} \in \mathbb{V}_l} \sigma^{(\boldsymbol{\xi})}_{l,m} \delta^{(\cdot)}_{x,\xi_x} \delta^{(\cdot)}_{y,\xi_y} \delta^{(\cdot)}_{z,\xi_z} \quad , \tag{24}$$

where $(\cdot)$ represents either approximation in (23) above. Centered approximations have no phase error, but a larger magnitude error relative to the minimal approximation. See Section IV-A.

Finally, the encoding equation (15) is approximated as

$$\delta^{(\cdot)}_{t,l} a^n_{l,m} = c^l \left(\delta^{(\cdot)}_{\mathbf{r},l,m} p\right)^n_{\mathbf{0}} \quad . \tag{25}$$

This can be implemented directly as a recursion for each $a^n_{l,m}$, employing previously computed approximations to derivatives of the acoustic field, deduced from the grid function $p^n_{\mathbf{q}}$, computed through scheme (16), and centered around the listener location at $\mathbf{q} = \mathbf{0}$, at time step n.

Computational cost is very low for these encoding methods, and scales with l^3. For the minimal scheme, for example, for $(l, m) = (0, 0)$, $(1, -1)$ and $(2, -2)$:

$$a^n_{0,0} = \sqrt{1/4\pi}\, p^n_{\mathbf{0}} \tag{26a}$$

$$a^{n+1}_{1,-1} = a^n_{1,-1} + \sqrt{3/4\pi}\lambda\left(p^n_{\mathbf{e}_2} - p^n_{\mathbf{0}}\right) \tag{26b}$$

$$a^{n+1}_{2,-2} = 2a^n_{2,-2} - a^{n-1}_{2,-2} + \sqrt{15/4\pi}\lambda^2\left(p^n_{\mathbf{e}_2+\mathbf{e}_1} - p^n_{\mathbf{e}_2} - p^n_{\mathbf{e}_1} + p^n_{\mathbf{0}}\right) \quad . \tag{26c}$$

These methods are the most basic available, but are susceptible to drift, due to the multiple time integrations which they approximate, from (15); this effect can be alleviated by using more refined integration schemes. See Section IV-B.

IV. Numerical Results

In this section, numerical results are presented. The scheme used is as defined by (16), with a time step $T = 1/44100$ s and $c = 344$ m/s, and a Courant number $\lambda = 1/\sqrt{3}$.

A. Numerical Directivity

Consider the encoding equation (25) under a plane wave solution (17), of angular frequency $\tilde{\omega}$, propagation direction $\boldsymbol{\gamma}$ and wavenumber $\tilde{k} = \tilde{k}(\tilde{\omega}, \boldsymbol{\gamma})$. $a^n_{l,m} = A^{(\cdot)}_{l,m}(\tilde{\omega}, \boldsymbol{\gamma})\, e^{i\tilde{\omega}nT}$ is the corresponding complex exponential under steady harmonic excitation, of amplitude A parameterized by γ.

The temporal shift operations s^+_t and s^-_t behave as multiplicative factors $e^{i\tilde{\omega}T}$ and $e^{-i\tilde{\omega}T}$, respectively, and spatial shift operations s^+_ν and s^-_ν, for $\nu = x, y, z$, as multiplicative factors $e^{i\tilde{k}\gamma_\nu X}$ and $e^{-i\tilde{k}\gamma_\nu X}$, respectively. The operators $\delta^{(\cdot)}_{\mathbf{r},l,m}$ and $\delta^{(\cdot)}_{t,l}$ then act as multiplicative factors

$$\delta^{(\cdot)}_{\mathbf{r},l,m} \to \hat{\delta}^{(\cdot)}_{\mathbf{r},l,m}(\omega, \boldsymbol{\gamma}) \qquad \delta^{(\cdot)}_{t,l} \to \hat{\delta}^{(\cdot)}_{t,l}(\omega) \quad . \tag{27}$$

The numerical directivity is then defined by

$$A^{(\cdot)}_{l,m}(\tilde{\omega}, \boldsymbol{\gamma}) = c^l \hat{\delta}^{(\cdot)}_{\mathbf{r},l,m}(\tilde{\omega}, \boldsymbol{\gamma}) / \hat{\delta}^{(\cdot)}_{t,l}(\tilde{\omega}) \quad . \tag{28}$$

This expression incorporates both the effects of numerical dispersion in the scheme, as well as inaccuracy in the approximation (25) used to extract spatially encoded signals.

Directivity plots are shown, for selected encoding coefficients up to third order in Figure 1, using both the minimal and centered encoding schemes. The minimal encoding scheme exhibits very low magnitude error, and a large phase error, and the centered encoding scheme shows a larger magnitude error, and no phase error (as is expected). The numerical frequency $\tilde{\omega}$ is chosen near the numerical cutoff in this case, at approximately $\tilde{\omega} = 0.7\tilde{\omega}_c$; for lower frequencies, the errors are reduced.

This article has been accepted for publication in a future issue of this journal, but has not been fully edited. Content may change prior to final publication. Citation information: DOI 10.1109/LSP.2019.2902509, IEEE Signal Processing Letters

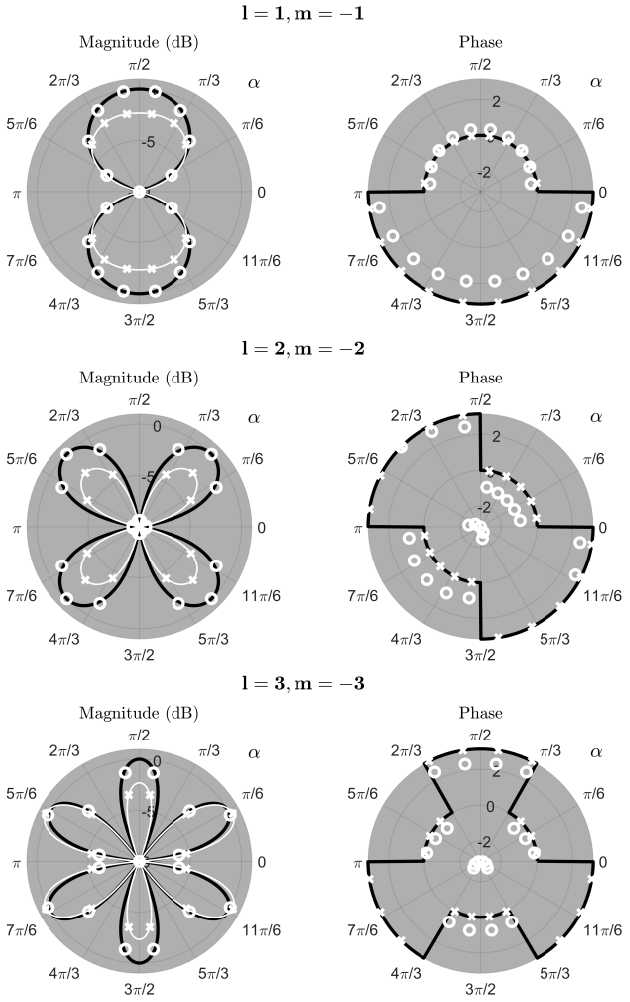

Fig. 1. Numerical directivity of approximations (25) used to obtain spatially encoded signals, for selected l, m pairs, as indicated. Here, the directivity shown is the expression given in (28), normalized by $\|Y_{l,m}\|_\infty$, and in the x, y plane, so $\boldsymbol{\gamma} = [\cos(\alpha), \sin(\alpha), 0]$, for angle α with $0 \leq \alpha < 2\pi$. Magnitude, in dB, is shown in the top row, and phase in the bottom row. In each case, the exact directivity is shown as a black line, the directivity due to a minimal order encoding by white circles, and due to a centered encoding by a white line with crosses. Directivity patterns are shown for a numerical frequency of $\tilde{\omega} = 2\pi \cdot 6000$ rad./sec.

B. Solution Drift

Volumetric wave-based methods inherently capture near-field behaviour. The encoding equation (15) relies on repeated time integration, and thus one should expect that low frequency temporal solution drift will occur (polynomial, of order $l-1$, for $l \geq 1$). The drift is a near-field effect—in particular, it is not a numerical effect, but a consequence of the definition of the encoding coefficients $a_{l,m}$. To illustrate this, consider a free-field setting, with a monopole source at coordinates $\mathbf{r}_s$, in m, relative to the listener position at $\mathbf{r} = \mathbf{0}$. The source is Gaussian signal of variance 10^{-4} s. See Figure 2, illustrating examples of encoded first- and second-order signals using scheme (25), and for source coordinates $\mathbf{r}_s = [0.2, 0.2, 0.2]$ and $\mathbf{r}_s = [1, 1, 1]$; the drift effect decreases with source distance (or as the listening position enters the far field).

Drift in encoded signals is obviously undesirable, and thus

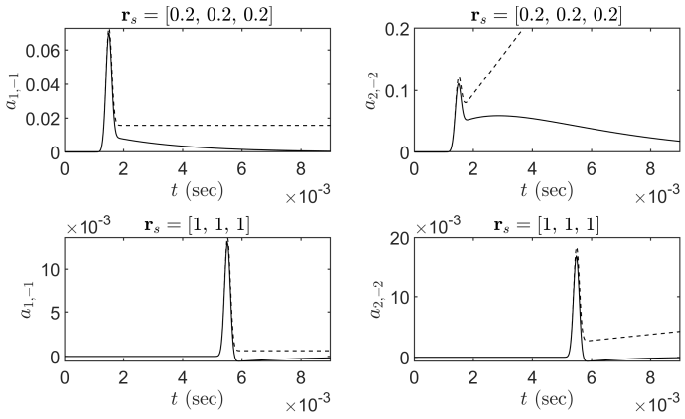

Fig. 2. Encoded signals $a_{l,m}$ under the basic scheme (25), exhibiting drift (dashed line) and under leaky integration (solid line), as defined in (29). Results are shown at source distances of $\mathbf{r}_s = [0.2, 0.2, 0.2]$ and $\mathbf{r}_s = [1, 1, 1]$, as indicated.

some additional filtering is required. A very simple approach is to employ leaky integration, effectively moving the lth order system poles away from DC. In the present context of time domain methods, one can replace the difference operators defined in (19) by the operators

$$\delta_t^+ = \frac{1}{T}\left(s_t^+ - e^{-2\pi f_0 T}\right) \quad \delta_t^- = \frac{1}{T}\left(1 - e^{-2\pi f_0 T} s_t^-\right) \quad (29)$$

for a given cutoff frequency f_0. See Figure 2, illustrating the suppression of drift in encoded signals using this approach, with $f_0 = 60$ Hz. The examples presented here are quite extreme—for sources a reasonable distance away from the listening point, the drift effect is greatly reduced.

V. Concluding Remarks

A procedure has been demonstrated here whereby spatially encoded signals may be extracted, locally, from a wave-based simulation at very low computational cost.

An important feature of the expression (15) is that is framed in the continuous space-time domain, and is separated into an approximation to the gradient followed by time integrations. Thus, the problem is reduced to approximation of spatial derivatives of the acoustic field, which can be performed for any grid arrangement (including unstructured grids). Here, the listener location is taken to lie at a grid location, but interpolated listener locations (possibly dynamic) are also possible, as in the case of source modeling [33]. There are clearly many ways to approximate spatial derivatives over a grid; very simple minimal but non-centered approximations

The problem of low-frequency solution drift has been briefly addressed here. It is not a consequence of the formulation presented here, and the analogous problem of filter designs with multiple poles at DC occurs in microphone array processing—see, e.g., [16]. A simple leaky integrator has been presented here, but far better designs are possible, allowing for better drift suppression with less distortion of the encoded signals over the audio range.

REFERENCES

[1] O. Chiba, T. Kashiwa, H. Shimoda, S. Kagami, and I. Fukai, "Analysis of sound fields in three dimensional space by the time-dependent finite-difference method based on the leap frog algorithm," *J. Acoust. Soc. Jpn.(J)*, vol. 49, pp. 551–562, 1993.

[2] D. Botteldooren, "Acoustical finite-difference time-domain simulation in a quasi-Cartesian grid," *J. Acoust. Soc. Am.*, vol. 95, no. 5, pp. 2313–2319, 1994.

[3] L. Savioja, T. Rinne, and T. Takala, "Simulation of room acoustics with a 3-D finite-difference mesh," in *Proc. Int. Comp. Music Conf.*, Århus, Denmark, Sep. 1994, pp. 463–466.

[4] S. Bilbao and J. O. Smith III, "Finite difference schemes and digital waveguide networks for the wave equation: Stability, passivity and numerical dispersion," *IEEE Transactions on Speech and Audio Processing*, vol. 11, no. 3, pp. 255–266, 2003.

[5] K. Kowalczyk and M. van Walstijn, "Room acoustics simulation using 3-D compact explicit FDTD schemes," *IEEE Trans. Audio, Speech, Language Proces.*, vol. 19, no. 1, pp. 34–46, 2011.

[6] B. Hamilton and S. Bilbao, "FDTD methods for 3-D room acoustics simulation with high-order accuracy in space and time," *IEEE Trans. Audio Speech Lang. Proces.*, vol. 25, no. 11, pp. 2112–2124, 2017.

[7] S. Bilbao, "Modeling of complex geometries and boundary conditions in finite difference/finite volume time domain room acoustics simulation," *IEEE Trans. Audio Speech Language Proces.*, vol. 21, no. 7, pp. 1524–1533, 2013.

[8] S. Bilbao, B. Hamilton, J. Botts, and L. Savioja, "Finite volume time domain room acoustics simulation under general impedance boundary conditions," *IEEE/ACM Trans. Audio Speech Language Proces.*, vol. 24, no. 1, pp. 161–173, 2016.

[9] D. Murphy, A. Kelloniemi, J. Mullen, and S. Shelley, "Acoustic modelling using the digital waveguide mesh," *IEEE Sig. Proc. Mag.*, vol. 24, no. 2, pp. 55–66, 2007.

[10] F. Georgiou and M. Hornikx, "Incorporating directivity in the Fourier pseudospectral time-domain method using spherical harmonics," *J. Acoust. Soc. Am.*, vol. 140, pp. 855–865, 2016.

[11] M. A. Gerzon, "Periphony: With-height sound reproduction," *J. Audio Eng. Soc.*, vol. 21, no. 1, pp. 2–10, 1973.

[12] M. A. Poletti, "Three-dimensional surround sound systems based on spherical harmonics," *J. Audio Eng. Soc.*, vol. 53, no. 11, pp. 1004–1025, 2005.

[13] F. Zotter and M. Frank, "All-round ambisonic panning and decoding," *J. Audio Eng. Soc.*, vol. 60, no. 10, pp. 807–820, 2012.

[14] M. Zaunschirm, C. Schörkhuber, and R. Höldrich, "Binaural rendering of ambisonic signals by head-related impulse response time alignment and a diffuseness constraint," *J. Acoust. Soc. Am.*, vol. 143, no. 6, pp. 3616–3627, 2018.

[15] J. Meyer and G. W. Elko, "Spherical microphone arrays for 3d sound recording," in *audio signal processing for next-generation multimedia communication systems*. Springer, 2004, pp. 67–89.

[16] B. Rafaely, *Fundamentals of Spherical Array Processing*. Springer, 2015.

[17] J. Sheaffer, M. van Walstijn, B. Rafaely, and K. Kowalczyk, "Binaural reproduction of finite difference simulations using spherical array processing," *IEEE/ACM Trans. Audio, Speech, Language Proces.*, vol. 23, no. 12, pp. 2125–2135, 2015.

[18] H. F. Olson, "Gradient microphones," *J. Acoust. Soc. Am.*, vol. 17, no. 3, pp. 192–198, 1946.

[19] M. Kolundzija, C. Faller, and M. Vetterli, "Spatiotemporal gradient analysis of differential microphone arrays," *J. Audio Eng. Soc.*, vol. 52, no. 1-2, pp. 20–28, 2011.

[20] A. Southern, D. Murphy, and L. Savioja, "Spatial encoding of finite difference time domain acoustic models for auralization," *IEEE Trans. Audio, Speech, and Language Processing*, vol. 20, no. 9, pp. 2420–2432, 2012.

[21] B. Støfringsdal and P. Svensson, "Conversion of discretely sampled sound field data to auralization formats," *J. Audio Eng. Soc.*, vol. 54, no. 5, pp. 380–400, 2006.

[22] D. M. M. Gómez, J. Astley, and F. M. Fazi, "Low frequency interactive auralization based on a plane wave expansion," *Appl. Sci.*, vol. 7, no. 6, p. 558, 2017.

[23] G. Dickins and R. Kennedy, "Towards optimal soundfield representation," in *Audio Engineering Society Convention Preprint*, Munich, Germany, May 1999, paper 4925.

[24] R. Mehra, L. Antani, S. Kim, and D. Manocha, "Source and listener directivity for interactive wave-based sound propagation," *IEEE Trans. Visualization Comp. Graphics*, vol. 20, no. 4, pp. 83–94, 2014.

[25] A. Pierce, *Acoustics: An Introduction to its Physical Principles and Applications*. Acoustical Society of America, 1991.

[26] E. G. Williams, *Fourier Acoustics: Sound Radiation and Nearfield Acoustical Holography*. Elsevier, 1999.

[27] B. A. Cray, V. M. Evora, and A. H. Nuttall, "Highly directional acoustic receivers," *J. Acoust. Soc. Am.*, vol. 113, no. 3, pp. 1526–1532, 2003.

[28] P. S. Cotterell, "On the theory of second-order soundfield microphone," Ph.D. dissertation, University of Reading, 2002.

[29] G. Dickins, "Soundfield representation, reconstruction and perception," M.Sc. thesis, The Australian National University, 2003.

[30] F. Zotter and A. U. Staackmann, "Simulation of room transfer functions with directivity patterns on the basis of modes," in *DAGA Fortschritte der Akustik*, 2017.

[31] S. Bilbao and B. Hamilton, "Higher-order accurate two-step finite difference schemes for the many dimensional wave equation," *J. Comp. Phys.*, vol. 367, pp. 134–165, 2018.

[32] R. Courant, K. Friedrichs, and H. Lewy, "Über die partiellen Differenzengleichungen de mathematischen Physik," *Mathematische Annalen*, vol. 100, pp. 32–74, 1928.

[33] S. Bilbao and B. Hamilton, "Directional sources in wave-based acoustic simulation," *IEEE/ACM Trans. Audio Speech Language Proces.*, 2018, in press.